


Article

Formation Mechanism and Control Technology of an Excavation Damage Zone in Tunnel-Surrounding Rock

Hongxian Fu ^{1,2}, Xiaoming Guan ³ , Chun Chen ⁴, Jianchun Wu ⁴, Qiqiang Nie ⁴, Ning Yang ^{3,*}, Yanchun Liu ³ and Junwei Liu ³

¹ Key Laboratory of Urban Underground Engineering of Ministry of Education, Beijing Jiaotong University, Beijing 100044, China

² College of Civil Engineering, Beijing Jiaotong University, Beijing 100044, China

³ College of Civil Engineering, Qingdao University of Technology, Qingdao 266520, China

⁴ China Railway No. 10 Engineering Group No. 3 Construction Co., Ltd., Hefei 230031, China

* Correspondence: nee_young@163.com

Abstract: Loosened rock circle is formed around the tunnel when the tunnel is constructed by the drilling and blasting method. The size of the loosened rock circle around the tunnel and the degree of internal rock fragmentation has an important influence on the support parameters, durability, and safety of the tunnel. Firstly, referencing an existing tunnel project, blasting tests using nonelectronic and electronic detonators were carried out to determine the influence of blasting construction on the scope of the rock loose circle and the degree of rock fragmentation. Then, a numerical simulation was used to study the contribution of the blasting impact and surrounding rock stress redistribution on the loosened rock circle around the tunnel. The results showed that the range of the loosened rock circle around the tunnel generated by the normal blasting of nonelectronic detonators was 1.5~2.3 m, and the wave velocity of the rock mass in the loosened rock circle around the tunnel decreased to 23~36%. The size of the loosened rock circle around the tunnel generated by the blasting impact was 0.66 m, accounting for 33% of the range of the loosened rock circle around the tunnel. The range of the loosened rock circle around the tunnel produced by electronic detonator blasting was 0~1.4 m. The wave velocity of the rock mass in the loosened rock circle around the tunnel decreased to 12~17%. The range of the loosened rock circle around the tunnel was approximately 60~76% of that of detonator blasting, and the broken degree of the surrounding rock in the loosened rock circle around the tunnel was small. The research results can provide a reference for the optimization design of preliminary support parameters of tunnels, such as anchors and steel arches in blasting construction.

Keywords: tunnel blasting; loosened rock circle; acoustic method; nonelectronic detonators; electronic detonator; control technology



Citation: Fu, H.; Guan, X.; Chen, C.; Wu, J.; Nie, Q.; Yang, N.; Liu, Y.; Liu, J. Formation Mechanism and Control Technology of an Excavation Damage Zone in Tunnel-Surrounding Rock. *Appl. Sci.* **2023**, *13*, 1006. <https://doi.org/10.3390/app13021006>

Academic Editors: Zhengzhao Liang, Bei Jiang and Nuwen Xu

Received: 28 November 2022

Revised: 7 January 2023

Accepted: 9 January 2023

Published: 11 January 2023



Copyright: © 2023 by the authors. Licensee MDPI, Basel, Switzerland. This article is an open access article distributed under the terms and conditions of the Creative Commons Attribution (CC BY) license (<https://creativecommons.org/licenses/by/4.0/>).

1. Introduction

The drilling and blasting methods are the most commonly used in the construction of rock tunnels. The protected surrounding rock is damaged, and its stress is redistributed after the rock within a tunnel outline is thrown out by the blasting load during excavation. The strength of the protected surrounding rock is reduced, and the original cracks of it are further widened to form a circle of loosened rock around the tunnel. This has a significant influence on the supporting parameters, durability, and structural safety of the tunnel.

The range, fragmentation degree, and permeability of loosened rock circles around the tunnel were extensively studied in terms of hydropower station chamber excavation, tunnel engineering, and waste storage cavern engineering [1]. Failure zone, fracture zone, and disturbance zone are formed in the surrounding rock after tunnel excavation. A large number of rocks are separated from the surrounding rock and become unstable bodies in the failure zone, and the surrounding rock generates microcracks or fissures in a fractured

zone. In the disturbance area, the stress of the surrounding rock and groundwater pressure has changed, yet other physical and mechanical properties of the surrounding rock have changed little [2].

At present, the range of loosened rock circles around the tunnel formed and their physical and mechanical properties after tunnel excavation have been studied by many scholars through theoretical analysis, field tests, and numerical simulation. A Russian scholar named Protodyakonov proposed the natural equilibrium arch theory and initiated a theoretical study of the loosened rock circle around a tunnel in the early 20th century. Subsequently, scholars established wedge theory, elastic medium theory, flexible medium theory, loose fracture theory, elastic–plastic medium theory, fracture zone diagram theory, and discontinuous zone theory [3]. Zhang et al. [4] and Jiang et al. [5] derived an analytical solution of the radius and stress of the plastic zone of a circular roadway based on elastic–plastic theory, the Drucker–Prager criterion, and the double-shear unified strength criterion. Wang et al. [6] and Wang et al. [7] derived an approximate solution to the boundary equation of the plastic zone of the surrounding rock of an unequal-pressure circular roadway based on the Hoek–Brown strength criterion and the Mohr–Coulomb strength criterion. Meng et al. [8] and Guan et al. [9,10] verified the elastic–plastic damage mechanical model of the surrounding rock and computed the plastic zone range. Based on elastic–plastic theory, many scholars have used different strength criteria and approved analytical methods to calculate the loosened rock circles around standard circular tunnels. Nevertheless, these computational results are problematic when meeting engineering needs. In order to obtain more practical theoretical analysis results, Ma et al. [11] deduced an analytical solution in which the plastic zone of a tunnel is controlled by the yield criterion during the failure process, and stress field changes were obtained in the plastic zone of the tunnel.

At the same time, the development of science and technology has brought a variety of advanced monitoring instruments, which have made outstanding contributions to the monitoring test of surrounding rock loose circles. Many scholars adopted multipoint displacement measurements, the seismic wave method, the geological radar method, and the borehole imaging method to study loose circles in tunnels. At present, the single-hole acoustic monitoring method [12] and the borehole acoustic monitoring method [13,14] are the most widely used methods to study the range of tunnels surrounding rock loose circles.

With improvements in computing ability and numerical algorithms, researchers have begun to use numerical simulations to calculate the range of loose circles. This method can fully combine the results of field monitoring and theoretical deduction, which is a hot topic in the research of the measuring range of loose circles [15]. Wei et al. [16], Han et al. [17], and Pan et al. [18,19] studied the deformation and failure characteristics of the surrounding rock by using particle flow and discrete element simulation methods that referenced a number of microfeature indicators, such as the microcrack field, crack propagation direction and final trend, and they provided a scientific explanation for the nature of many physical phenomena. In addition to blasting factors, the existence of in situ stress can also lead to stress fracture cycles in a tunnel excavation section. Siren et al. [20] conducted research to distinguish between blasting and stress-induced fracture zones.

Blasting technology has a great influence on the range and mechanical properties of tunnels surrounding rock loose circles. The tunnel blasting method can be categorized as either ordinary blasting, smooth blasting, or micro-vibration blasting. Through field tests and research, the loose circle formed by ordinary blasting has been deemed the largest, followed by smooth blasting, and the smallest circle is created by micro-vibration blasting [21]. However, there are few studies on the loose ring under the combined use of various blasting methods. Zhou et al. [22] believed that multiple blasting methods only produced cumulative damage at the cracks or fissures and increased the displacement at the joint surface, and the loose ring size depended on the maximum burst. Liu et al. [14] and Li et al. [23] found that multiple explosions expanded the loose circle from 2.8 m to 3.2 m through the acoustic wave method and borehole peeping method and increased the degree of rock breakage, and the damage degrees of sidewalls and vaults can increase

by 36~50% and 47~55% in loose circles, respectively. Ji et al. [24] used field tests and finite element simulations to study the changes in the cumulative damage zones of tunnel-surrounding rock under multiple excavation and blasting conditions, and the damage degrees of the surrounding rock were sorted, divided, and summarized. Yang et al. [25,26] studied the difference between the blasting vibration on a tunnel surface and the blasting vibration inside the surrounding rock through field tests and the differences between the vibration peaks and dominant frequencies on the tunnel surface and the interior of the surrounding rock.

At present, there is no unified and clear definition of a loose tunnel circle, and the disturbance zone, plastic zone, and loose circle are often muddled. The technical construction specification for rock foundation excavation in hydraulic structures stipulates that the change rate of wave velocity greater than 10% after blasting is the criterion of rock mass failure. This study used this standard to determine the loose circle of a tunnel. The loosening circle is formed under the dual actions of blasting and stress redistribution in the surrounding rock. However, the contribution of the two to the final loose circle remains unclear. In this study, referencing the construction of a tunnel, blasting construction tests of nonelectric detonators and electronic detonators are carried out. The vibration velocity and the range of the loose circle produced by the two blasting methods were tested. The field test data and numerical simulation method were used to explore the influence of the surrounding rock stress redistribution and blasting load on the range of the loose circle. The results show that the use of electronic detonators is more conducive to the protection of tunnel surrounding rock than non-electric detonators and can significantly reduce the rock damage range.

2. General Information of the Project

The research background project is Renhechang Tunnel, which is an important project on the Chongqing-Huaihua Railway and the total length is 4734 m. The rock layer is mainly mudstone with sandstone with some developed joints, and water seepage often occurs during excavation.

In order to study the formation mechanism of the loose circle produced by tunnel blasting, tunnel nonelectric detonator blasting, and electronic detonator blasting tests are carried out in a section. The new railway tunnel passes underneath an existing highway tunnel in this section. The distance between the new tunnel and the existing tunnel is 30~31 m, and the length of the underpass is 70 m. The tunnel of this section passes through a geological section of mudstone clamp sandstone, and the surrounding rock grade is IV. The physical and mechanical properties of the surrounding rock of the tunnel are shown in Table 1.

Table 1. Material property parameters of main stratum types of excavated tunnels.

| Geotechnical Name | Unit Weight γ (kN/m ³) | Cohesion C (kPa) | Angle of Internal Friction φ (°) | Basic Bearing Capacity σ_0 (kPa) |
|-------------------|---|--------------------|--|---|
| Gravel soil | 21 | | 20 | 100 |
| Mollison | 18.5 | 12 | 7 | 100 |
| Silty clay | 19 | 20 | 15 | 150 |
| Mudstone clamp | 22 | | 35 | 300 |
| Sandstone | 23 | | 45 | 450 |

3. Blasting and Vibration Tests

Firstly, the first blasting damage test of the surrounding rock was carried out with nonelectric detonators. The hole arrangement and initiation sequence are shown in Figure 1, and the blasting parameters are shown in Table 2. Because the section passes through an operating highway tunnel, the blasting vibration test points are arranged in the operating highway tunnel and above the excavation face. The specific monitoring points are arranged

in Figure 2. The y -direction blasting vibration velocity received by the three-direction velocity sensor is the largest according to the spatial position of the sensor and the explosion source, so these tests focus on the y -direction vibration velocity. The blasting vibration velocity waveform is shown in Figure 3.

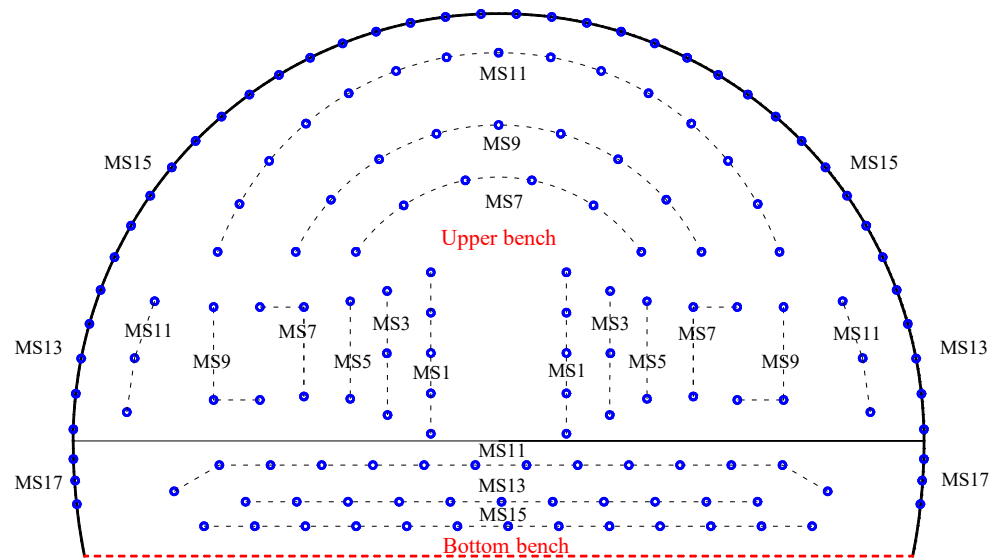


Figure 1. The hole arrangement and initiation sequence of nonelectric detonator blasting in the test. Note: The marked MS represents the detonator delay time series. The holes connected by dotted lines are in the same delay sequence and represent simultaneous initiation.

Table 2. Details of blasting holes and explosive parameters.

| Bench | Name of the Boreholes | Number of Holes | Borehole Depth (m) | Single Hole Charge (kg) | Detonator Segment | Subsection Charge (kg) |
|-------------------------------|-----------------------|-----------------|--------------------|-------------------------|-------------------|------------------------|
| The arch part of upper bench | Auxiliary hole | 6 | 3 | 1.0 | MS7 | 6.0 |
| | Auxiliary hole | 9 | 3 | 1.0 | MS9 | 9.0 |
| | Auxiliary hole | 15 | 3 | 1.0 | MS11 | 15.0 |
| | Peripheral hole | 28 | 3 | 0.6 | MS15 | 16.8 |
| The lower part of upper bench | Cutting hole | 10 | 4.5 | 2.0 | MS1 | 20.0 |
| | Auxiliary hole | 6 | 4 | 1.8 | MS3 | 10.4 |
| | Auxiliary hole | 4 | 4 | 1.6 | MS5 | 6.4 |
| | Auxiliary hole | 12 | 3 | 1.2 | MS7 | 7.2 |
| | Auxiliary hole | 6 | 3 | 1.0 | MS9 | 6.0 |
| | Auxiliary hole | 6 | 3 | 1.0 | MS11 | 6.0 |
| | Peripheral hole | 10 | 3 | 0.6 | MS13 | 6.0 |
| Bottom bench | Auxiliary hole | 12 | 3 | 1.8 | MS11 | 21.6 |
| | Auxiliary hole | 13 | 3 | 1.8 | MS13 | 23.4 |
| | Auxiliary hole | 14 | 3 | 1.8 | MS15 | 25.2 |
| | Peripheral hole | 6 | 3 | 0.6 | MS17 | 3.6 |
| Total | | 157 | | | | 182.6 |

Then, the blasting test of surrounding rock damage was carried out by using electronic detonators. In order to ensure that the two tests have high contrast, the same hole arrangement of the two tests is ensured, as shown in Figure 4. The hole charge weight and blasting vibration test point arrangements are the same as those for nonelectric detonator blasting. The vibration velocity waveform of the electronic detonators is shown in Figure 5.

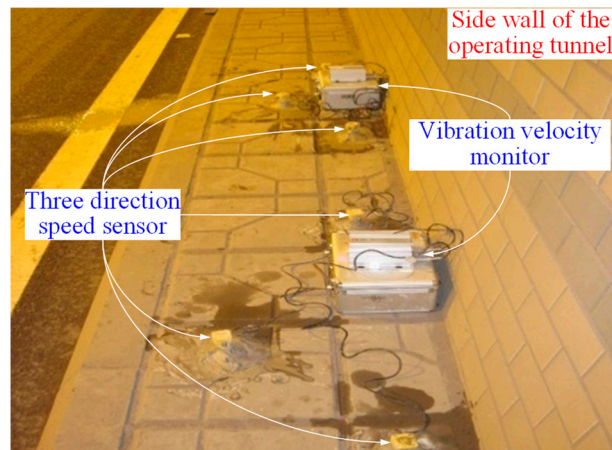


Figure 2. Vibration velocity monitoring points in operating tunnel above excavation face.

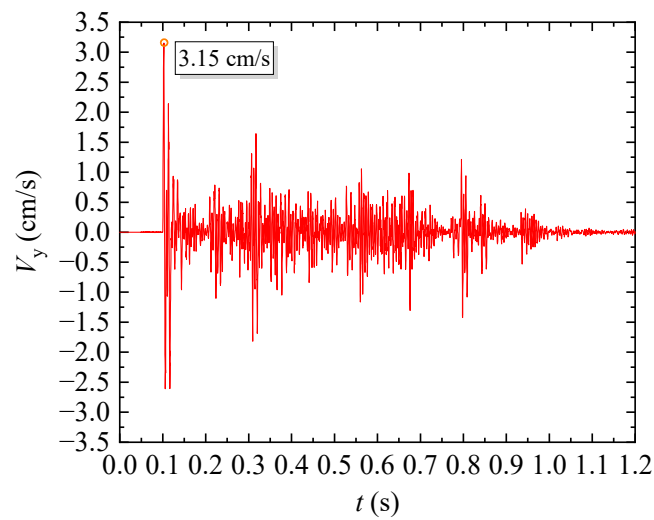


Figure 3. Vibration waveform of tunnel nonelectric detonator blasting.

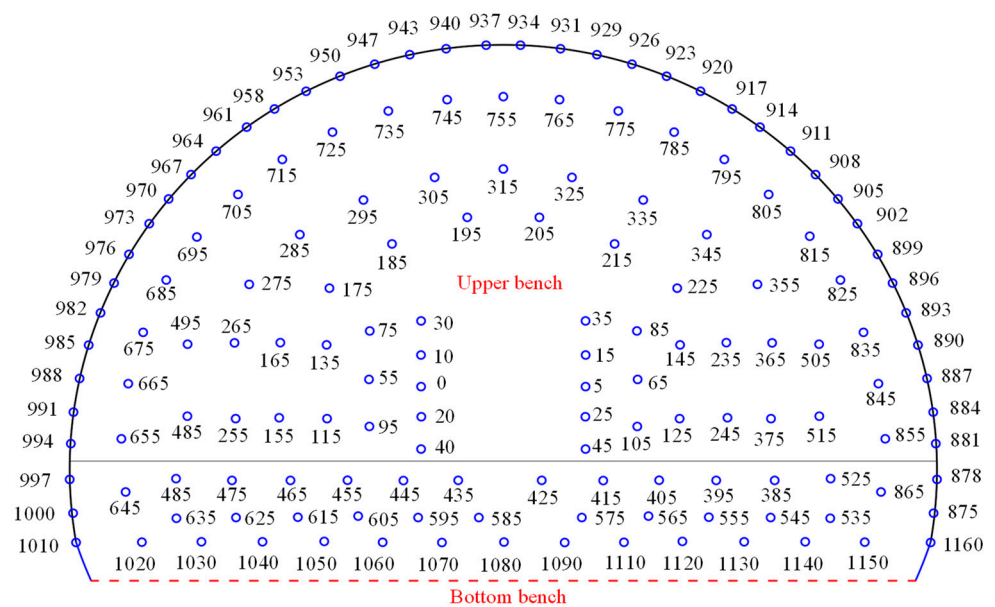


Figure 4. The blasting hole arrangement and initiation sequence of tunnel electronic detonators.

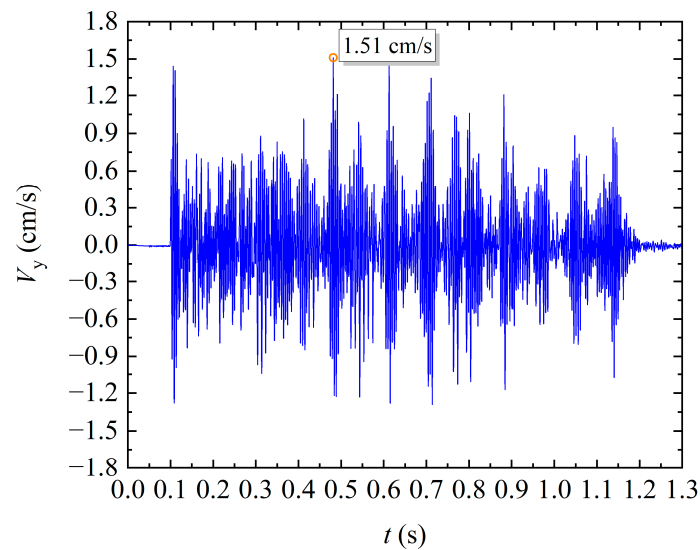


Figure 5. Blasting vibration velocity waveform of tunnel electronic detonators.

The maximum vibration velocity is 3.15 cm/s when the nonelectric detonators are used, and the maximum vibration velocity is reduced to 1.51 cm/s after the electronic detonator test, as shown in Figures 3 and 5, respectively. The maximum vibration velocity caused by electronic detonators is about 52.1% lower than that caused by nonelectric detonators, and the decrease is obvious. An important factor affecting the damage of surrounding rock is the maximum vibration velocity generated by cutting blasting. However, the maximum vibration velocity is randomly generated in a blast hole when using electronic detonators. Therefore, vibration reduction measures such as drilling empty holes to reduce cut blasting do not have advantages in the use of electronic detonator initiation. Another important reason is that the nonelectric detonator initiation delay accuracy is not easy to control. The delay parameter error of the design based on the burning velocity of the explosive is large, which makes it necessary to detonate multiple holes at the same time. On the contrary, the delay accuracy of electronic detonators has been significantly improved. It can realize the sequential initiation of single hole without considering the influence of cumulative error. In this way, the amount of explosive detonated at the same time is significantly less than that of nonelectric detonator. The technical improvement has led to the control of the possible higher vibration velocity from the source.

The vibration velocity monitoring results of the two tests are analyzed. It is found that the peak particle velocity produced by cutting blasting is the largest in the nonelectric detonator test. The vibration velocities generated by subsequent blastholes are significantly reduced. The continuous high vibration velocity of electronic detonators may have greater adverse effects on the surrounding rock. Therefore, the method of monitoring the loose range of surrounding rock on site is adopted to explore this hypothesis.

4. Monitoring the Loose Circle after Two Blasting Tests

The longitudinal wave velocity of the surrounding rock was monitored by the conventional single-hole test method using an RSM-SY5 acoustic detector after tunnel blasting excavation. The compressional wave velocity of the tunnel-surrounding rock had a good correlation with the degree of surrounding rock breakage. The longitudinal wave velocity of surrounding rock decreases with the increase in its fracture development degree. The conventional single-hole acoustic wave testing method is shown in Figure 6, and the layout of the test holes is shown in Figure 7. A simple trolley and pneumatic drill were used to drill the holes. According to field test experience, the hole depths were 4.0~4.4 m, and the hole diameters were 40 mm. The blasthole was set perpendicular to the tunnel wall as much as possible to meet the loose ring test requirements [27,28]. The drilling and testing process is shown in Figure 8. Due to the relatively developed cracks in the surrounding

rock, the test holes in the vault could not be filled with water, resulting in the test holes not being tested.

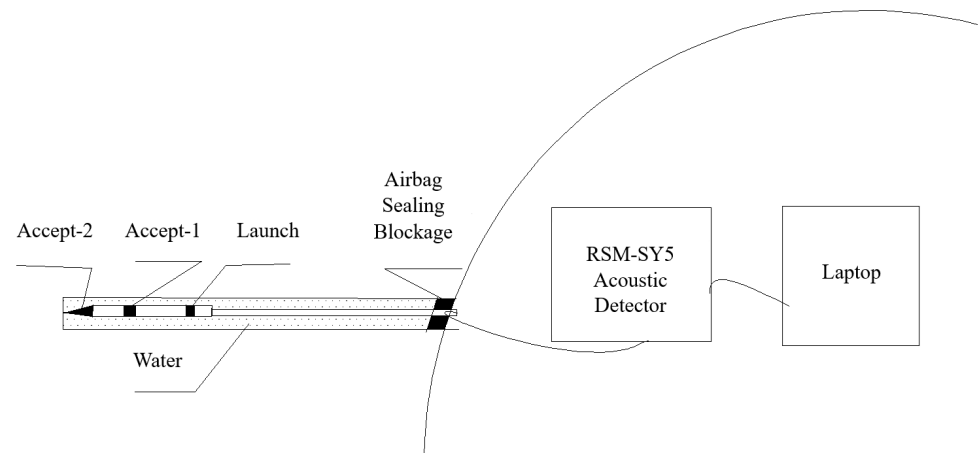


Figure 6. Schematic diagram of single-hole test by acoustic method.

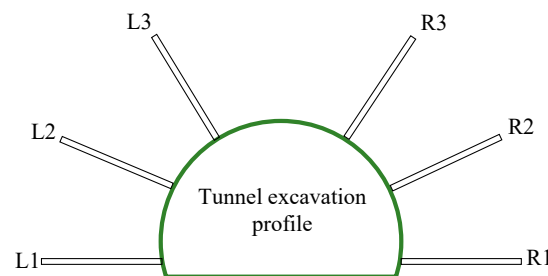


Figure 7. Schematic diagram of test hole layout.

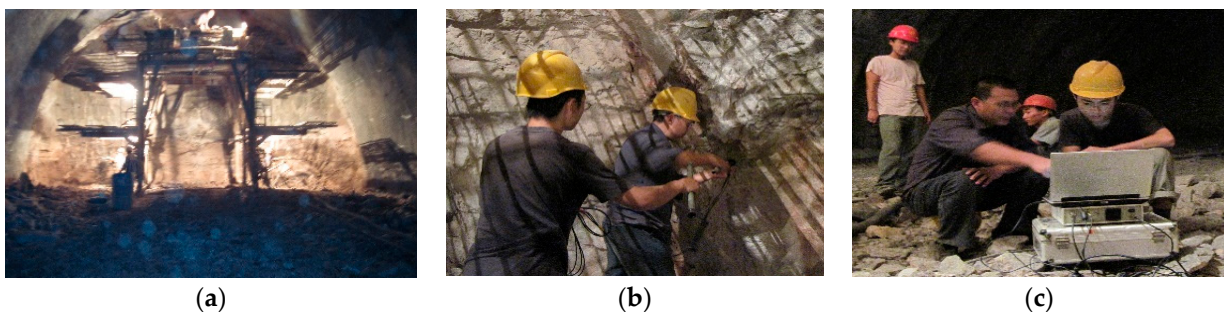


Figure 8. Field test of the loose circle. (a) Use support trolley to assist drilling; (b) install monitoring sensors; (c) observe the monitoring results.

At present, there is no unified and clear definition of a loose tunnel circle. The technical code for the construction of rock foundation excavation engineering of hydraulic structures [29] notes that the change rate of wave velocity greater than 10% after blasting is the criterion of rock mass failure. Firstly, two footage sections with similar surrounding rock properties were first selected. In order to ensure the accuracy of the monitoring results, priority will be given to test work after blasting. Each monitoring test lasted nearly 12 h. The test analysis of the tunnel loose circle range excavated by nonelectric and electronic detonator blasting is shown in Figures 9 and 10. The position where the first rapid increase of wave velocity was monitored can be considered as the boundary position of the loose circle, and the blue dotted line is used as the auxiliary line to mark the boundary position of the loose circle. The shape of the loose circle during nonelectric and electronic detonator blasting is shown in Figure 11. The properties of the loose circle are shown in Table 3.

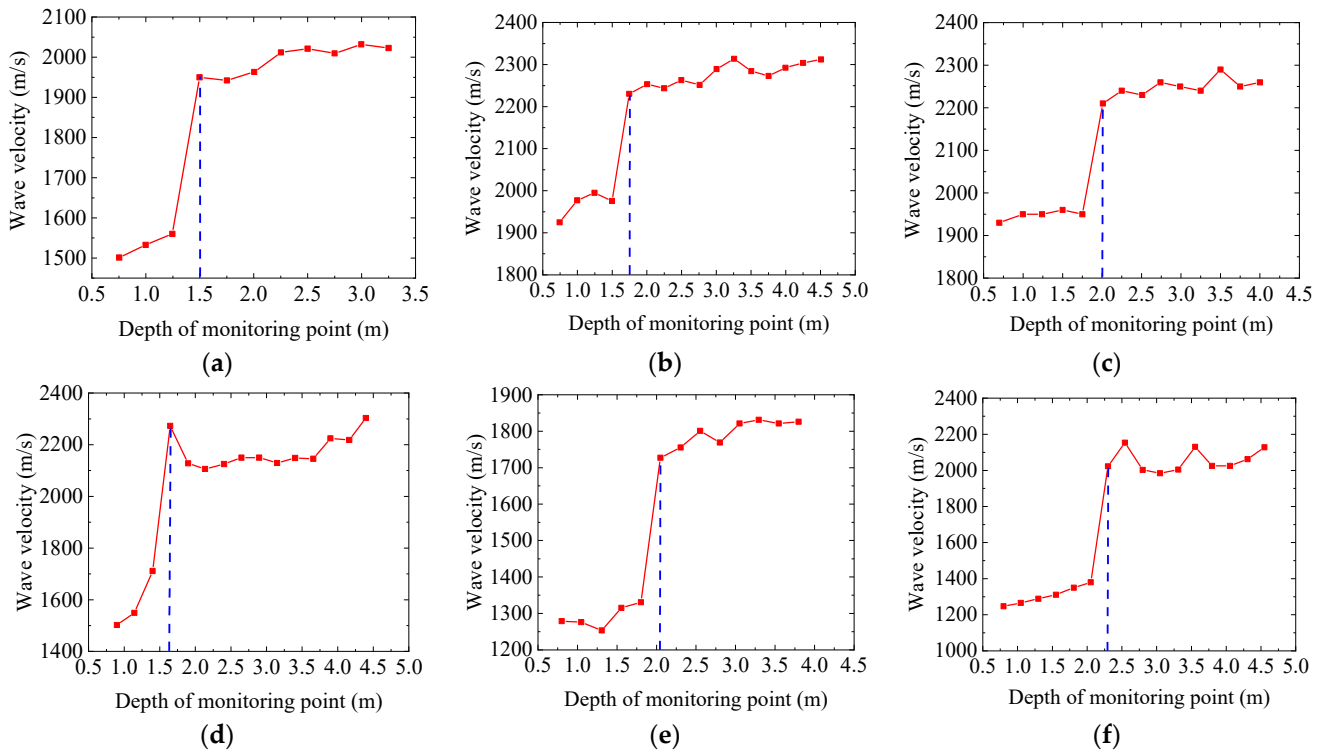


Figure 9. Variation in the longitudinal wave velocity of the surrounding rock with the test hole depth during tunnel non-electric detonator blasting excavation. (a) R1, (b) R2, (c) R3, (d) L1, (e) L2, and (f) L3.

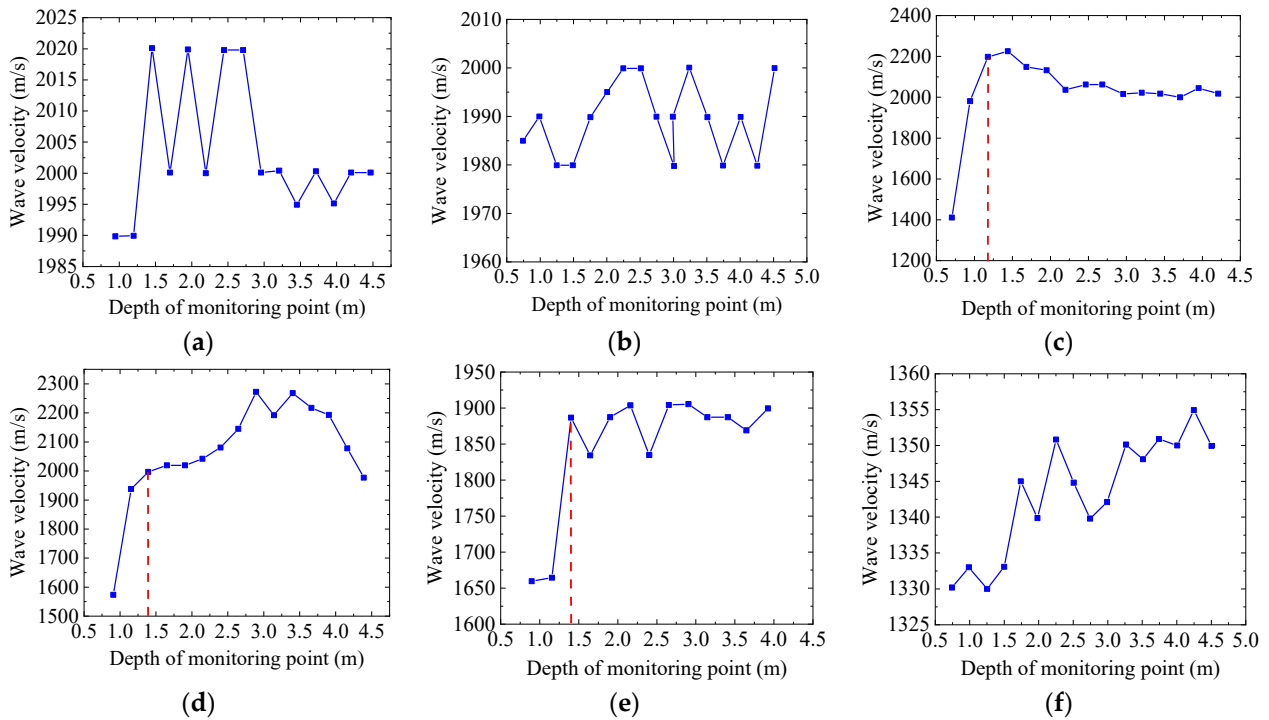


Figure 10. Variation in the longitudinal wave velocity of the surrounding rock with the test hole depth during tunnel electronic detonator blasting excavation. (a) R1, (b) R2, (c) R3, (d) L1, (e) L2, and (f) L3.

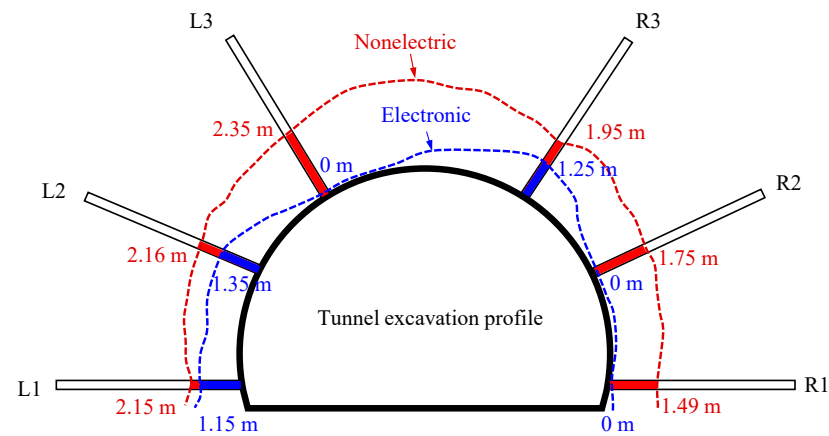


Figure 11. Schematic diagram of a loose circle during tunneling by nonelectric and electronic detonator blasting.

Table 3. Property parameters of the tunnel nonelectric and electronic detonator blasting loose circle.

| Test Holes | Loosening Range (m) | | Reduction Degree of Longitudinal Wave Velocity of Surrounding Rock | |
|------------|---------------------|------------|--|------------|
| | Nonelectric | Electronic | Nonelectric | Electronic |
| R1 | 1.49 | 0 | 22% | 2% |
| R2 | 1.75 | 0 | 14% | 2% |
| R3 | 1.95 | 1.25 | 13% | 16% |
| L1 | 2.15 | 1.15 | 33% | 17% |
| L2 | 2.16 | 1.35 | 28% | 20% |
| L3 | 2.35 | 0 | 40% | 2% |

Contrastive analysis of loose circles produced by nonelectric detonator blasting and electronic detonator blasting in tunnels. Nonelectric detonators and electronic detonators were used in field tests, while ensuring the similarity of surrounding rock properties at the two blasting footages as much as possible.

(1) Fragmentation degree of the rock mass in a loose circle. In terms of loose range of surrounding rock, the depth of the loose circle caused by the nonelectric detonator was 1.49~2.35 m, and the depth caused by the electronic detonator was 0~1.35 m. The loose range caused by nonelectric detonators is significantly larger than that of electronic detonators in each radial direction, as shown in Figure 11. The serious damage depth of 2.35 m is avoided in the L3 direction, and the reduction in other directions is basically above 1 m. Two sections with the same surrounding rock properties cannot be found in the field test, and the random distribution of joint fissures cannot be avoided. There are a large number of joint fissures in the left tunnel wall and the right tunnel spandrel of the test section using electronic detonators after field investigation. The rock is mixed with a weak sand layer, and the water seepage phenomenon is obvious. This leads to the phenomenon of large damage depth at the L1, L2, and R3 positions in the electronic detonator test results. The electronic detonators can reduce the damage depth of more than 1 m, which can significantly reduce the use of supporting bolts, resulting in greater economic benefits, according to the construction experience. At the same time, it also avoids the construction process of post grouting reinforcement. More importantly, it can ensure the safety and stability of the tunnel after blasting.

(2) In addition, the use of electronic detonators not only reduces the depth of the damage range but also has a significant effect on retaining the integrity of the surrounding rock. The wave velocity of the rock mass in the loose circle caused by the nonelectric detonator decreases to 13~40%, and that of the rock mass in the loose circle caused by

the electronic detonator decreases to 16~20%, as shown in Table 3. The use of electronic detonators can significantly weaken the reduction of longitudinal waves in the surrounding rock. It is conducive to giving full play to the supporting role of the original surrounding rock and ensuring the stability of the excavated tunnel.

The field tests consume a lot of human and material resources and delay the construction period. It cannot be carried out on a large scale. Therefore, in order to further study the differences between electronic and nonelectric detonators in tunnels surrounding rock damage, it is necessary to use finite element software for further research and analysis.

5. Finite Element Analysis and Removal of Stress Redistribution Factors

Large finite element software FLAC3D has been widely used in geotechnical and underground engineering. It can be analyzed by the “mixed discrete method” when simulating plastic failure. It can provide more accurate and reasonable results than the ordinary discrete integration method. Therefore, FLAC3D software was used for numerical simulation in this study.

The tunnel excavation section area was approximately 150 m² with a span of 14.7 m and a height of 12.5 m. To avoid the influence of the model boundary effect, in the numerical model, the distance between the tunnel center axis and the left and right boundaries was greater than four times the tunnel span, the distance between the tunnel center axis and the upper and lower boundaries was also greater than three times the tunnel span. The excavation footage was 3 m. The whole calculation model was 120 m wide and 100 m high, with 49,152 units in total. The models are shown in Figures 12 and 13.

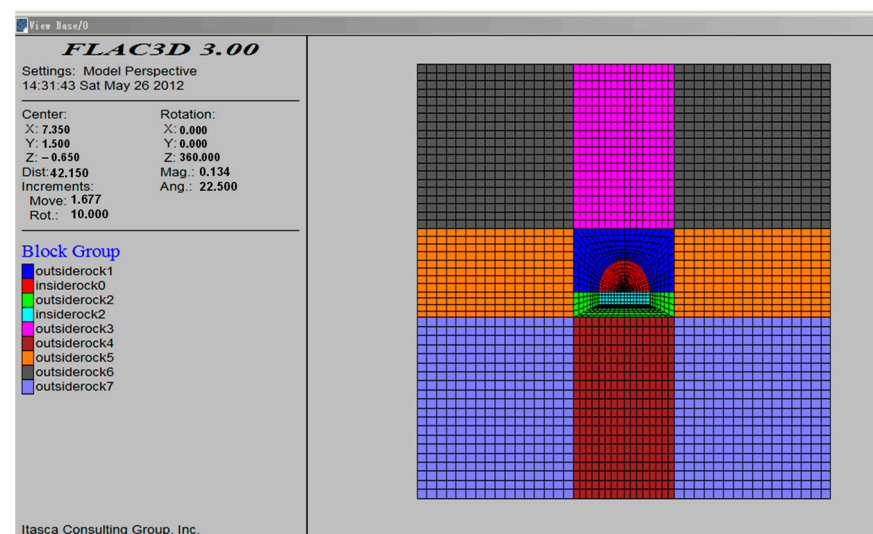


Figure 12. Plane view of finite element model.

Based on the physical and mechanical parameters of the surrounding rock, the final parameter values were as follows after trial calculation by referring to relevant manuals [29]: Elasticity modulus $E = 10$ GPa. Poisson’s ratio $\nu = 0.3$. Frictional angle $\varphi = 35^\circ$. The cohesive force of the surrounding rock was 1×10^5 Pa. The tensile strength of the surrounding rock was 3×10^5 Pa.

In the FLAC3D calculation, the rock mass deformation parameters were the volume modulus (K) and shear modulus (G). Therefore, the elastic modulus or deformation modulus (E) and Poisson’s ratio (ν) must be transformed into volume modulus (K) and shear modulus (G), and the transformation formula is as Equations (1) and (2).

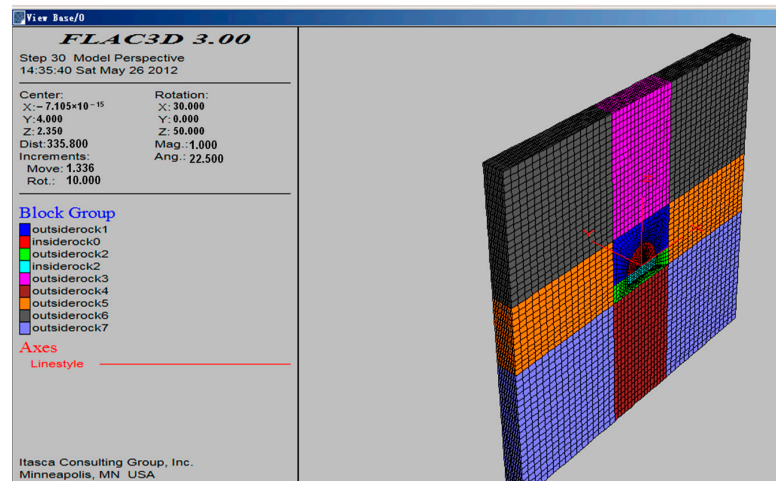


Figure 13. Three-dimensional view of finite element model.

$$K = \frac{E}{3(1 - 2\mu)} \tag{1}$$

$$G = \frac{E}{2(1 + \mu)} \tag{2}$$

The bulk modulus K and shear modulus G of the model can be calculated by Equations (3) and (4).

Bulk modulus:

$$K = \frac{E}{3(1 - 2\mu)} = 8.33 \times 10^9 \text{ (Pa)} \tag{3}$$

Shear modulus:

$$G = \frac{E}{2(1 + \mu)} = 3.85 \times 10^9 \text{ (Pa)} \tag{4}$$

In the FLAC3D dynamic calculation, four kinds of dynamic loads can be input: acceleration time history, velocity time history, displacement time history, and stress time history. The dynamic load input of this simulation adopted the monitored blasting vibration velocity time-history curve since the actual particle vibration velocity data were measured by field test. This effectively ensures that the numerical simulation calculations are as consistent as possible with the field blasting tests.

The monitored vibration velocity in Figures 3 and 5 was transformed into the vibration velocity time-history curve required by FLAC3D, as shown in Figures 14 and 15.

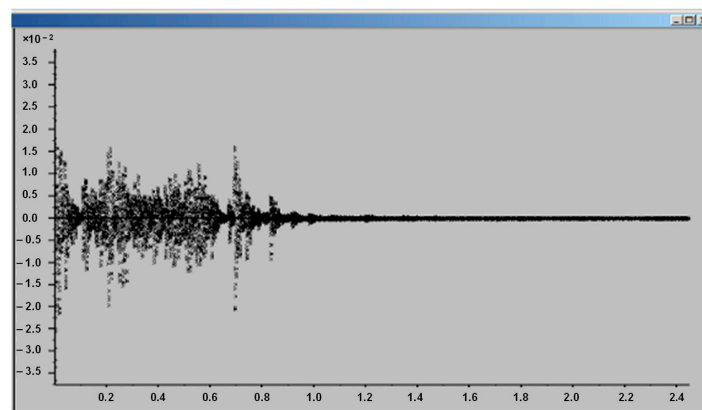


Figure 14. Data after nonelectric detonator vibration test and transition.

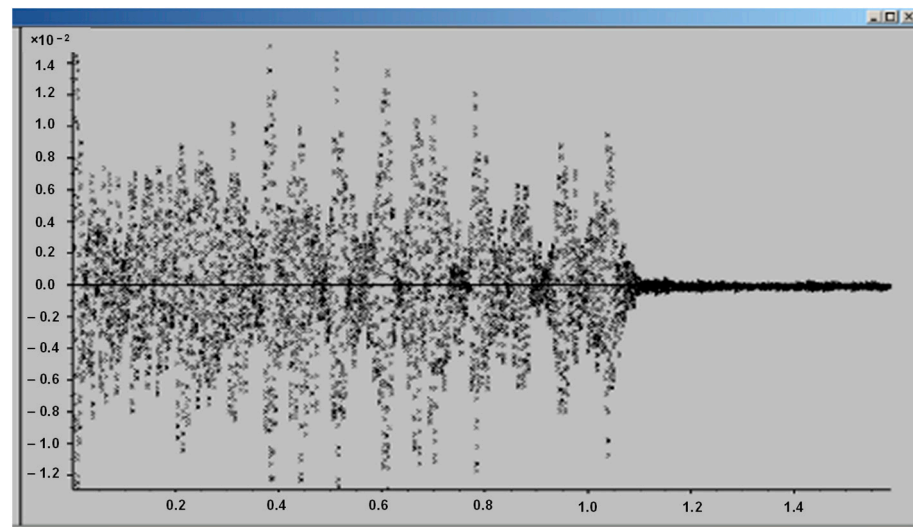


Figure 15. Data after electronic detonator vibration test and transition.

The loose circles of the tunnel blasted by nonelectric detonators and electronic detonators were obtained by numerical calculation, as shown in Figures 16 and 17. The blue elements in the figures represent the undamaged surrounding rock. The green, brown and red elements represent the damage of surrounding rock, and the damage degree decreases in turn.

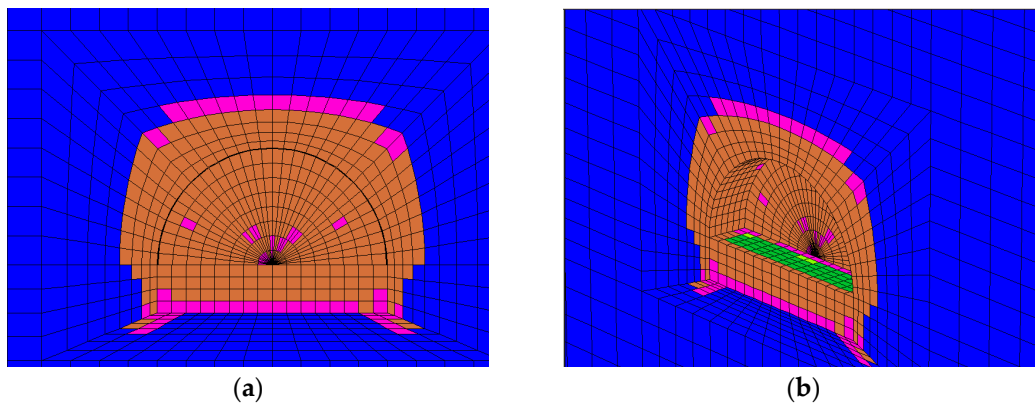


Figure 16. Numerical calculation of loose circle for nonelectric detonator blasting excavation. (a) Plane view; (b) 3D view.

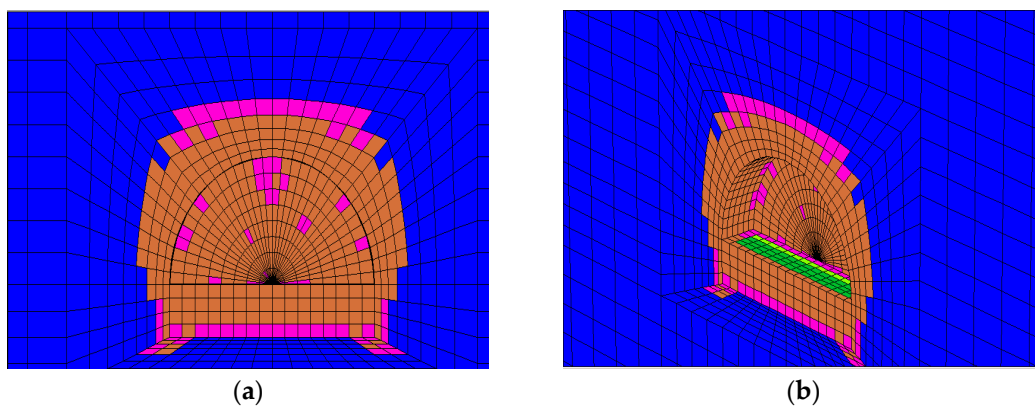


Figure 17. Numerical calculation of loose circle for electronic detonator blasting excavation. (a) Plane view; (b) 3D view.

In order to combine the field tests, the numerical simulation is carried out according to the actual blasting footage of 3 m. The nonelectric detonator test caused 137.33 m³ surrounding rock unit failure in the footage through the statistical data in Table 4, and the average thickness of the surrounding-rock loose circle is shown in Table 5. The average damage depth of the entire excavation section caused by explosive initiation can be obtained by dividing the surface area of the excavation profile within the footage length. The average failure depth of surrounding rock damage caused by the nonelectric detonator test is close to 2 m. This is basically consistent with the results monitored in the field test, which verifies the correctness of the numerical model. Similarly, 104.86 m³ surrounding rock units failed in the electronic detonator results, and the average failure depth was 1.514 m. The calculated average depth of electronic detonators is obviously smaller than that of nonelectric detonators. The finite element simulation can ensure that the material properties of surrounding rock are the same in two times of blasting. The surrounding rock is assumed to be a homogeneous material without joint fissure. Therefore, the calculated results of nonelectric and electronic detonators are smaller than those of field tests, which is reasonable. This further validates the irregularity of the damage profile in Figure 11 in Section 4. It shows that in the area where the electronic detonator test is used, the joint fissures at the left wall and right spandrel positions of the tunnel have a great influence on the test results. It significantly reduces the blast resistance of surrounding rock.

Table 4. The average thickness of the loose ring calculated by simulation.

| Computational Model | Excavation Footage (m) | Yield Volume (m ³) | Average Thickness (m) |
|-----------------------|------------------------|--------------------------------|-----------------------|
| Nonelectric detonator | 3 | 137.33 | 1.980 |
| Electronic detonator | 3 | 104.86 | 1.514 |

Table 5. The average thickness of the loose ring in the comparative test.

| Computational Model | Loading Situation | Yield Unit Volume (m ³) | Loose Ring Average Thickness (m) | Thickness of Loose Ring Due to Blasting Load (m) | Influence of Blasting Action on Loose Ring |
|-----------------------|-------------------|-------------------------------------|----------------------------------|--|--|
| Nonelectric detonator | Yes | 137.33 | 1.98 | 0.66 | 33% |
| | No | 91.34 | 1.32 | | |
| Electronic detonator | Yes | 104.86 | 1.51 | 0.20 | 13% |
| | No | 91.34 | 1.32 | | |

The field blasting tests can only monitor the final damage range of surrounding rock because of the instantaneity of explosion. In fact, the loose circle of surrounding rock is generated by the double effects of stratum stress redistribution caused by excavation and blasting load impact. Here, the finite element simulation method is used to analyze these two factors in depth. The numerical simulation consists of two cases. One was to simulate the blasting effect without applying a dynamic load, and the other was to simulate the blasting effect while applying a dynamic load. The two simulation results are shown in Table 5.

From Table 5, the following conclusions can be drawn:

(1) The thickness of the loose ring was approximately 1.32 m without considering the blasting load when the tunnel was excavated by conventional nonelectric detonator blasting. The thickness of the loose ring generated by the blasting load was approximately 0.66 m. The final thickness of the loose ring was 1.98 m. It can be considered that the extent of the loose circle generated by the redistribution of surrounding rock stress accounts for 67% of the final loose circle. The range of the loose circle produced by the blasting load accounts for 33% of the final loose circle range. Although the thickness of the rock loose

circle caused by surrounding rock excavation accounts for the main part, the influence of the blasting load is also significant.

(2) The thickness of the loose ring was approximately 1.32 m without considering the blasting load when the tunnel was excavated by electronic detonator blasting. The thickness of the loose ring produced by the blasting load was approximately 0.20 m. The final thickness of the loose circle was 1.51 m. It could be considered that the range of the looseness circle generated by the stress redistribution of the surrounding rock accounts for 87% of the final loose circle. The range of the loose circle produced by the blasting load accounts for 13% of the final loose range. The damage proportion of electronic detonator blasting load to surrounding rock loose circles is much lower than that of nonelectric detonators. Therefore, it can be considered that the damage degree of explosives controlled by electronic detonators to surrounding rock is much smaller than that of nonelectric detonators because of their better delay and smaller explosive detonating quality each time.

6. Recommendations and Limitations

This study explored the damaging effect of the use of electronic detonators and nonelectric detonators on the protected surrounding rock. The monitoring and calculation results of damage range and rock crushing degree show that a nonelectric detonator has a positive effect on the protection of surrounding rock. Its application in practical engineering can be embodied in the following two aspects: Firstly, in terms of the loose range of surrounding rock, the thickness of the loose circle of surrounding rock caused by the electronic detonator is 1 m less than that of the nonelectric detonator on average, so the length of the anchors can be shortened appropriately when setting the primary support. In terms of the degree of rock fragmentation, the maximum acoustic velocity attenuation caused by an electronic detonator is only half of that of a nonelectric detonator. Therefore, the amount of shotcrete can be reduced, and the spacing of steel arches can be appropriately increased when setting the primary support. This study provided a reference for the optimization design of primary support parameters of the tunnel after blasting, which is helpful in reducing construction costs.

However, the current testing methods cannot accurately divide the failure zone, the crack zone, and the plastic zone, so the size of the loose circle in the test is not uniform. Although specifications [29] provide blasting damage standards, a rock mass is judged to be damaged if the change rate of the rock mass wave velocity before and after blasting is greater than 10%. In some cases, the surrounding rock in the loose circle fractured but still retains high stability. In addition, the influence of initial surrounding rock fissures is not excluded in this study. Therefore, further classification criteria of surrounding rock loose circles and the influence of initial surrounding rock fissures will be considered in future studies.

7. Conclusions

In this study, the damage of protected surrounding rock by using an electronic detonator and a nonelectric detonator in tunnel blasting was compared. The advantages of using an electronic detonator to protect surrounding rock were quantified through field monitoring and numerical simulation. The research results can provide a reliable reference for the design of controlled blasting and the determination of support parameters in tunnel excavation engineering. Some valuable conclusions are drawn from this study:

(1) In the surrounding grade IV rock, when the blasting footage was 3 m, the nonelectric detonators were used for normal construction, and the range of the loose circle was 1.5~2.3 m. The resulting loose circle ranged from 0 m to 1.4 m after the nonelectric detonators were changed to electronic detonators under the condition that the distance between the holes and the amount of charge remained unchanged. The range of the loose circle produced by the blasting of the tunnel electronic detonator was approximately 60~76% of that of the nonelectric detonator blasting, and the surrounding rock in the loose circle was less broken.

(2) When nonelectric detonators were used for blasting, the impact of the blasting load on the loose ring was approximately 33% due to the large blasting load. The small blasting load of the single-hole electronic detonator leads to an approximately 13% effect of the blasting load on the loose circle.

(3) The above studies show that the use of electronic detonators for the protection of surrounding rock has a beneficial effect. The preliminary support parameters of the tunnel can be optimized after excluding the interference of initial surrounding rock fissures. When using electronic detonators, the specific optimization parameters can be expressed as reducing the length of the anchor, increasing the steel arch spacing, and reducing the amount of shotcrete.

Author Contributions: Conceptualization, H.F., X.G. and C.C.; methodology, X.G., J.W. and Q.N.; software, N.Y.; validation, J.W., C.C. and H.F.; formal analysis, J.L.; investigation, Q.N.; resources, H.F.; data curation, Y.L.; writing—original draft preparation, H.F. and N.Y.; writing—review and editing, N.Y., Y.L. and J.L.; visualization, Y.L.; supervision, X.G. All authors have read and agreed to the published version of the manuscript.

Funding: This research was funded by the Service Safety and Intelligent Maintenance of Rail Transit Operation Tunnels (2022JBXT007), the General Program of Shandong Natural Science Foundation of China (ZR2022ME043), and the General Program of National Natural Science Foundation of China (51978356).

Institutional Review Board Statement: Not applicable.

Informed Consent Statement: Not applicable.

Data Availability Statement: The data used to support the findings of this study are included within the article.

Conflicts of Interest: The authors declare no conflict of interest.

References

1. Kwon, S.; Lee, C.; Cho, S.; Jeon, S.; Cho, W. An investigation of the excavation damaged zone at the kaeri underground research tunnel. *Tunn. Undergr. Space Technol.* **2009**, *24*, 1–13. [\[CrossRef\]](#)
2. Hadgu, T.; Kalinina, E.; Wang, Y.F. Investigations of effect of underground excavations using hydrologic and tracer transport modeling. *Tunn. Undergr. Space Technol.* **2022**, *127*, 104577. [\[CrossRef\]](#)
3. Chen, G.H.; Zou, J.F.; Min, Q.; Guo, W.J.; Zhang, T.Z. Face stability analysis of a shallow square tunnel in non-homogeneous soils. *Comput. Geotech.* **2019**, *114*, 103112. [\[CrossRef\]](#)
4. Zhang, X.; Song, H.W.; Yan, X. Analysis of Tunneling Stability Using Classic and Extended Drucker-Prager Model. *Chin. J. Undergr. Space Eng.* **2018**, *6*, 1652–1657.
5. Jiang, F.; Wang, G.; He, P.; Hou, B.; Zhang, S.B.; Sun, S.Q.; Zheng, C.C.; Wu, Y. Mechanical failure analysis during direct shear of double-joint rock mass. *Bull. Eng. Geol. Environ.* **2022**, *81*, 410. [\[CrossRef\]](#)
6. Wang, W.J.; Han, S.; Dong, E.Y. Boundary equation of plastic zone in roadway surrounding rocks considering supporting effect and its application. *J. Min. Saf. Eng.* **2021**, *38*, 749–755. [\[CrossRef\]](#)
7. Wang, R.; Yuan, D.Y.; Zhang, J.Z.; Yang, J. Analysis on broken zone of surrounding rock in tunnel based on Hoek-Brown strength criterion. *J. Saf. Sci. Technol.* **2017**, *13*, 58–63. [\[CrossRef\]](#)
8. Meng, L.; Gao, Z.N.; Meng, X.R. Elasto-plastic analysis of circular roadway surrounding rocks under consideration of rock damage. *J. Saf. Sci. Technol.* **2013**, *9*, 11–16. [\[CrossRef\]](#)
9. Guan, X.M.; Zhang, L.; Wang, Y.W.; Fu, H.X.; An, J.Y. Velocity and stress response and damage mechanism of three types pipelines subjected to highway tunnel blasting vibration. *Eng. Fail. Anal.* **2020**, *118*, 104840. [\[CrossRef\]](#)
10. Guan, X.M.; Zhang, L.; Wang, L.M.; Fu, H.X.; Yu, D.M.; Chen, G.; Ding, Y.; Jiang, W.L. Blasting vibration characteristics and safety standard of pipeline passed down by tunnel in short distance. *J. Cent. South Univ. (Sci. Technol.)* **2019**, *50*, 11. [\[CrossRef\]](#)
11. Ma, Y.C.; Lu, A.Z.; Cai, H.; Zeng, X.T. Analytical solution for determining the plastic zones around two unequal circular tunnels. *Tunn. Undergr. Space Technol.* **2022**, *120*, 104267. [\[CrossRef\]](#)
12. Dong, F.T. *The Supporting Theory Based on Broken Rock Zone and Its Application Technology*; Coal Industry Press: Beijing, China, 2001.
13. Hu, K.H. Application Research on Rapid Surrounding Rock Classification and Loose Circle Test. *Railw. Constr. Technol.* **2022**, *3*, 22–26. [\[CrossRef\]](#)
14. Liu, Y.S.; Zhu, S.Y.; Yang, X.L. Study on Damage Accumulation and Broken Rock Zone Range of Surrounding Rock of Large Span Chamber caused by Multiple Blasts. *Blasting* **2022**, *39*, 9–15, 35. [\[CrossRef\]](#)

15. Zhao, X.; Dai, Z.J.; Li, R.H.; Tao, L.J. Earthquake Mitigation Measures for Tunnels Considering Loosen-zone in Surrounding Rock. *J. Beijing Univ. Technol.* **2022**, *46*, 1027–1038. [[CrossRef](#)]
16. Wei, J.B.; Wang, S.M.; Zhao, Z.; Li, D.L. Numerical Study of Damage to Rock Surrounding an Underground Coal Roadway Excavation. *Adv. Civ. Eng.* **2020**, *16*, 8863289. [[CrossRef](#)]
17. Han, H.Y.; Fukuda, D.; Liu, H.Y.; Salmi, E.F.; Sellers, E.; Liu, T.J.; Chan, A. Combined finite-discrete element modelling of rock fracture and fragmentation induced by contour blasting during tunnelling with high horizontal in-situ stress. *Int. J. Rock Mech. Min. Sci.* **2020**, *127*, 104214. [[CrossRef](#)]
18. Guan, X.M.; Yang, N.; Zhang, W.J.; Li, M.G.; Liu, Z.L.; Wang, X.H.; Zhang, S.L. Vibration response and failure modes analysis of the temporary support structure under blasting excavation of tunnels. *Eng. Fail. Anal.* **2020**, *136*, 106188. [[CrossRef](#)]
19. Pan, C.; Li, X.; Li, J.C.; Zhao, J. Numerical investigation of blast-induced fractures in granite: Insights from a hybrid LS-DYNA and UDEC grain-based discrete element method. *Geomech. Geophys. Geo-Energy Geo-Resour.* **2021**, *7*, 1–18. [[CrossRef](#)]
20. Siren, T.; Kantia, P.; Rinne, M. Considerations and observations of stress-induced and construction-induced excavation damage zone in crystalline rock. *Int. J. Rock Mech. Min. Sci.* **2015**, *73*, 165–174. [[CrossRef](#)]
21. Salum, A.H.; Murthy, V. Optimising blast pulls and controlling blast-induced excavation damage zone in tunnelling through varied rock classes. *Tunn. Undergr. Space Technol.* **2019**, *85*, 307–318. [[CrossRef](#)]
22. Zhou, H.; Xiao, M.; Yang, Y.; Liu, G.Q. Seismic Response Analysis Method for Lining Structure in Underground Cavern of Hydropower Station. *KSCE J. Civ. Eng.* **2019**, *23*, 1236–1247. [[CrossRef](#)]
23. Li, R.L.; Qu, H.L.; Zhou, T.; Zhou, C.T. An experimental investigation on fatigue characteristics of granite under repeated dynamic tensions. *Int. J. Rock Mech. Min. Sci.* **2022**, *158*, 105185. [[CrossRef](#)]
24. Ji, L.; Zhou, C.B.; Lu, S.W.; Jiang, N.; Gutierrez, M. Numerical Studies on the Cumulative Damage Effects and Safety Criterion of a Large Cross-section Tunnel Induced by Single and Multiple Full-Scale Blasting. *Rock Mech. Rock Eng.* **2021**, *54*, 6393–6411. [[CrossRef](#)]
25. Yang, J.H.; Lu, W.B.; Li, P.; Yan, P. Evaluation of Rock Vibration Generated in Blasting Excavation of Deep-buried Tunnels. *KSCE J. Civ. Eng.* **2018**, *22*, 2593–2608. [[CrossRef](#)]
26. Yang, J.H.; Cai, J.Y.; Yao, C.; Li, P.; Jiang, Q.H.; Zhou, C.B. Comparative Study of Tunnel Blast-Induced Vibration on Tunnel Surfaces and Inside Surrounding Rock. *Rock Mech. Rock Eng.* **2019**, *52*, 1–15. [[CrossRef](#)]
27. Fu, H.X.; Zhao, Y.; Xie, J.S. Test Analysis on the Broken Rock Zone of the Surrounding Rock Blasting for Railway Double-Line Tunnel. *China Railw. Sci.* **2010**, *31*, 54–55. [[CrossRef](#)]
28. Fu, H.X.; Wang, L.N.Y.; Zhao, Y.; Shen, Z.; Zhang, C.P.; Li, Y.Z. Comparison of Excavation Damage Zones Resulting from Blasting with Nonel Detonators and Blasting with Electronic Detonators. *Rock Mech. Rock Eng.* **2014**, *47*, 809–816. [[CrossRef](#)]
29. *DL/T 5389-2007; Construction Technical Specifications on Rock-Foundation Excavation Engineering of Hydraulic Structures*. China Water Resources and Hydropower Press: Beijing, China, 2007.

Disclaimer/Publisher’s Note: The statements, opinions and data contained in all publications are solely those of the individual author(s) and contributor(s) and not of MDPI and/or the editor(s). MDPI and/or the editor(s) disclaim responsibility for any injury to people or property resulting from any ideas, methods, instructions or products referred to in the content.